doi:10.14311/ppt.2025.3.214
Plasma Physics and Technology **12**(3):214–218, 2025

ARC CONDUCTANCE DECAY AS A PERFORMANCE INDICATOR FOR THERMAL INTERRUPTION IN CO_2/O_2 MIXTURE

P. Pietrzak*, M. Muratović, M. Seeger, J. T. Engelbrecht, T. Votteler

Hitachi Energy Research, 5405 Baden-Dättwil, Switzerland

* pawel.pietrzak@hitachienergy.com

Abstract. Arc conductance decay is a well-established performance indicator for thermal interruption in SF_6, with a narrow range of known limit values. It is also shown that conductance decay can also serve as a performance indicator in CO_2-based mixtures, although different limit values for successful thermal interruption apply. In this publication, values of arc conductance 200 ns before current zero are presented for a large number of experiments performed in CO_2/O_2 90/10 mixture under short line fault-like conditions. These measurements are used to establish limit values for the CO_2/O_2 mixture, and to investigate the pressure dependence of conductance decay.

Keywords: high-voltage circuit breaker, SF6 alternatives, Conductance Decay.

1. Introduction

Over the past few decades, SF_6 has been the main switching and insulating medium used in high-voltage circuit breakers (HVCB). Several indicators of thermal interruption performance were established for SF_6 HVCBs, including post-arc current (amplitude and duration), arc voltage extinction peak, and conductance decay. The most commonly used metric of conductance decay is the instantaneous value of arc conductance measured 200 ns before current zero (CZ), which is referred to as G200. It has been shown that interruption likelihood has an inverse relationship with the G200 value, and that limit values of G200 are largely the same over a wide range of conditions and designs. In the literature there are many reports showing what G200 value must be achieved in an SF_6 HVCB to successfully interrupt the current in a short line fault type test.

Smeets *et al.* [1] presented limit values of G200 for a great number of HVCBs with ratings ranging from 72 kV to 550 kV. The reported limit values ranged from 0.81 mS to 3 mS. Seeger *et al.* [2] suggests that for successful thermal interruption in SF_6, G200 should be below 1 mS, and for alternative CO_2-based gases G200 should have values lower by a factor of two.

There have already been a few publications presenting limit values for G200 for one specific test object with CO_2/O_2 gas mixtures [3, 4], which are in line with the suggestion from Seeger. In this publication, for the first time a range of limit values for CO_2/O_2 based HVCBs is presented. These values were determined from a large number of tests performed over the course of 18 measurement series, where each series was performed with a different test object variant, comprising 155 measured G200 values in total.

In addition, an attempt at correlating G200 values with the pressure dependence of thermal interruption performance is presented and compared with previous work by Christen *et al.* [5] and Engelbrecht *et al.* [6].

2. Methods

Measurements were performed with a number of test object variants with varying interruption zone geometry - one measurement series per variant. The test object was stressed with current and voltage supplied by a synthetic test circuit, shown schematically in Figure 1. The synthetic circuit contains a high current circuit and a high voltage circuit, which respectively provide the high current during the contact opening phase and the required conditions around current zero, i.e. the $\mathrm{d}i/\mathrm{d}t$ before current zero and the transient recovery voltage(TRV) after current zero. The synthetic circuit provides short-line fault (SLF) L90-like conditions. TRV rise defined by a fixed 450Ω surge impedance, meaning that the voltage rise directly depends on the current $\mathrm{d}i/\mathrm{d}t$, and follows the L90 conditions up to first line peak. Example current and voltage waveforms are shown in Figure 2. All test objects were filled with 9.2 bar absolute of CO_2/O_2 90/10 gas mixture.

To determine the conductance near current zero, accurate, high resolution measurements of current and voltage are needed.

The current measurement is particularly challenging in such conditions, as 200 ns before CZ it is in the range of single digit A, while a few ms earlier it was in the high double digit kA range. To accurately measure the small currents under these conditions, the post-arc current (PAC) measurement system proposed by Votteler *et al.* [7], which is capable of measuring currents down to 200 mA was used. This system is based on the parallel connection of a shunt resistor and amplified voltage divider, with anti-parallel diodes

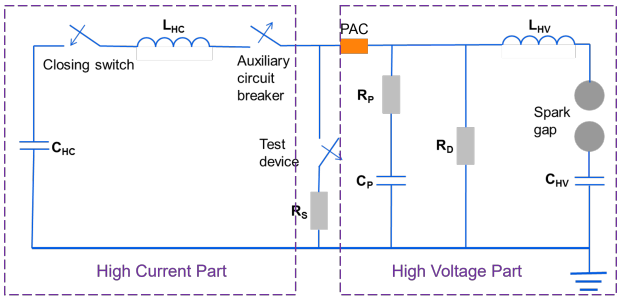

Figure 1. Schematic of the synthetic circuit.

limiting the output voltage during the high current phase. Over the course of the measurements the linear response range of the PAC system was adjusted several times, however for most of the measurements it was in the range of −3.5 A to 3.5 A, where the sensitivity was maximized.

The voltage signal was corrected for the influence of stray inductance using the prospective $\mathrm{d}i/\mathrm{d}t$. The PAC measurement system was located on the high voltage side of the high voltage circuit. At this measurement location, the current flowing into the shunt capacitance of the circuit breaker is also measured, which can be significant during the high $\mathrm{d}u/\mathrm{d}t$ phase around current zero. Therefore the current signal was corrected for parasitic capacitance using the corrected voltage signal.

Limit values of G200 were calculated separately for each measurement series using a logistic regression classification algorithm proposed previously for this calculation [3]. The limit value is defined as the conductance corresponding to a 50 % probability of successful current interruption. An example of the G200 limit determination with this method is shown in Figure 3. The overall limit value was calculated as the mean of all limit values from the individual measurement series.

Example PAC measurements and calculated conductance decay curves for one measurement series are shown in Figure 5.

2.1. Pressure dependence calculation

Christen *et al.* showed that the breaking performance ($\mathrm{d}i/\mathrm{d}t_{limit}$) scales approximately with the square root of the blow pressure at current zero [5]. "Blow pressure at current zero" will be referred to as "pressure" to keep it concise. This dependence is nearly independent of the gas. Additionally Habedank *et al.* [8] showed that $\ln(R)$ scales with $\mathrm{d}i/\mathrm{d}t_{limit}$, where R is the arc resistance close to current zero. This means the following (G is the arc conductance):

$$\ln R \sim \sqrt{p}, \tag{1}$$

$$R \sim e^{\sqrt{p}}, \tag{2}$$

$$\frac{1}{G} \sim e^{\sqrt{p}}, \tag{3}$$

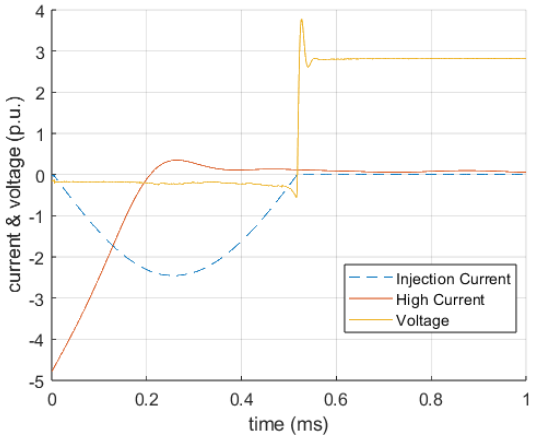

Figure 2. Example measurement of single shot with the successful arc interruption - zoom to the current zero area. Transient recovery voltage follows the SLF L90 only up to first line peak.

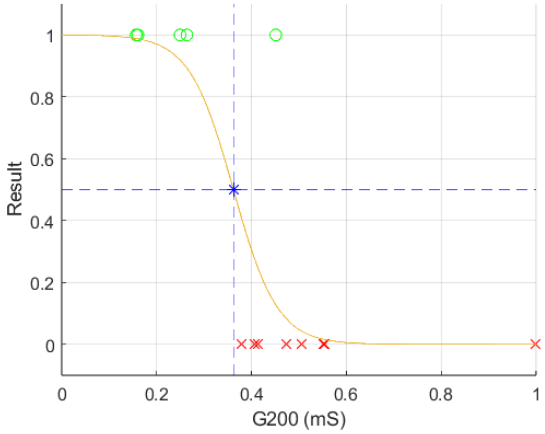

Figure 3. Logistic regression classification algorithm usage to find the G200 limit value. Red crosses - failure, green circles - success, blue asterisk - 50 % probability of success which is consider as threshold value.

$$G \sim \frac{1}{e^{\sqrt{p}}}. \tag{4}$$

Therefore, the following dependency between arc conductance 200 ns before current zero (G200) and pressure at current zero (p_{cz}) can be assumed:

$$G_{200} = \frac{C}{e^{\sqrt{p_{\mathrm{cz}}}}}, \tag{5}$$

where the proportionality constant C gives an indication for pressure-reduced thermal interruption performance (depending on the design). C was determined for each individual measurement, and then a mean value was taken as the coefficient for the whole measurement series.

Given the sensitivity of G200 to $\mathrm{d}i/\mathrm{d}t$, only measurements with similar prospective $\mathrm{d}i/\mathrm{d}t$ ($\pm$ 0.15 A/µs) are considered in this pressure dependence evaluation.

Engelbrecht *et al* [6] also investigated the pressure dependence of the thermal interruption limit in CO_2,

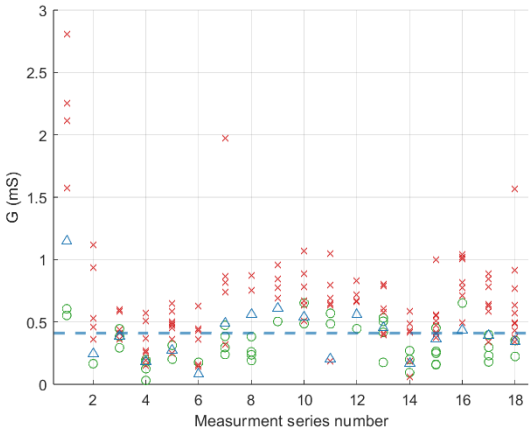

. Red crosses - failure, green circles - success, blue triangle - threshold for given measurement series, blue dashed line - overall threshold.

Figure 4. G200 values for all measurements, with varying di/dt and pressure

and found a different scaling exponent of $\frac{2}{3}$ was the best fit to their measurements. Following Eqs (1)–(4) using this pressure scaling exponent yields:

$$G_{200} \sim \frac{1}{e^{p_{cz}^{2/3}}}, \tag{6}$$

for the relationship between G200 and pressure

To determine whether the measurement results show better agreement with Eq. (5) or (6), a fit to the following equation was performed for the results of each measurement series:

$$G_{200} = \frac{1}{e^{n+p_{cz}^{m}}}, \tag{7}$$

where n and m are fitting parameters describing the proportionality constant and pressure scaling exponent, respectively.

Blow pressure was measured with a transient pressure sensor located in the volume upstream from the arcing zone.

3. Results

3.1. G200 limit

3.1.1. Results

In Figure 4, G200 values for all 155 shots from 18 measurement series are presented and categorized by shot outcome, i.e. failures where the arc was not extinguished are distinguished from successes in which the arc was extinguished. Limit values of G200 range from 0.09 mS to 0.61 mS, with one outlier at 1.15 mS. The mean limit value from all measurement series was found to be 0.42 mS, with a standard deviation of $\sigma = 0.24$ mS.

The evolution of conductance decay and PAC values over the course of one measurement series is shown in Figure 5. It is visible that over the course of the experiment there is a trend of increasing conductance

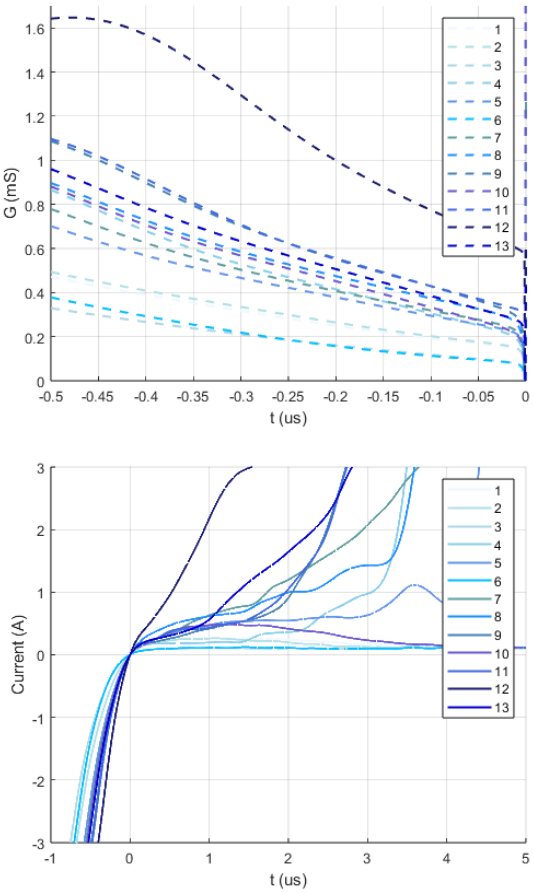

Figure 5. Conductance decay (top) and post arc current (bottom) in a course of one measurement series numbered chronologically.

values, leading to higher post-arc current and more thermal failures later in the measurement series.

3.1.2. Discussion

The measured limit values span a smaller range than those presented by Smeets *et al.* [1] for SF_6 circuit breakers. This could be related to intrinsic properties of the gas mixtures, or due to smaller variations between the investigated test objects. Similar to previous publications on the G200 limit of CO_2-based gases, overlap regions are observed where for an intermediate range of G200 values both success and failures can occur [3, 4].

In the literature, a G200 limit value of 0.24 mS was obtained for CO_2/O_2 90/10 under similar SLF L90-like stresses, in a test object with highly controllable and reproducible conditions [3]. This study reported additional G200 limit values for similar CO_2-based mixtures that all fell in a range close to 0.4 mS. These limit values were obtained using a different approach - keeping constant pressure at CZ across all tests and adjusting di/dt, as opposed to the approach presented here, where most of the measurements were performed within a narrow di/dt range but a wide range of pressures at CZ. Despite this difference, the two limit

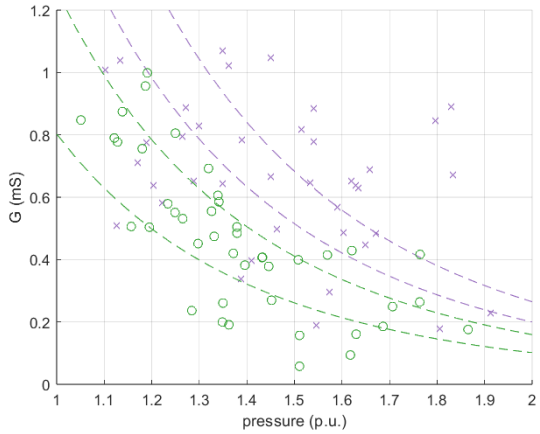

Figure 6. G200 values in function of the pressure, green and purple color represent two groups of measurements, circles and crosses show single measurements, dashed line are fit based on equation 5 for the measurement series with the highest and lowest C coefficient.

values are in general agreement considering the mutual uncertainties, suggesting that limit values of G200 can be established independently of test object, blow pressure, and testing approach.

The results presented here confirm that G200 can be used as a thermal interruption performance indicator in CO_2 based gas mixtures, and should be compared against a lower limit value than was used for SF_6 [3].

3.2. G200 pressure scaling

3.2.1. Results

In Figure 6, results from different measurement series are divided into two groups with similar C coefficients. Fits of Equation 5 are also plotted, showing the lowest and highest C from each group, thereby forming an envelope representing $\sqrt{p}$ scaling that can be compared with the results.

In Figure 7, fits to the same equation are compared with fits to Equation 7. The two groups from Figure 6 are plotted separately here, with the purple group representing high C (i.e. high G200) values and the green group representing low C (i.e. low G200) values, respectively. For the first group with high G200 values, the fit of the pressure scaling exponent m tends to be lower than the $e^{p^{0.5}}$ given by Equation 5, suggesting a dependence closer to $e^{p^{0.3}}$. For the measurement series with lower values of G200, most closely follow the proposed $\sqrt{p}$ scaling exponent, with two showing slight deviations - one with a higher and one with a lower value for m.

The group of measurement series with lower G200 values, which showed closer agreement, are plotted with separate fits for every test series in Figure 8.

3.2.2. Discussion

The fits to Equation 5 showed good agreement for the measurement series with lower measured G200

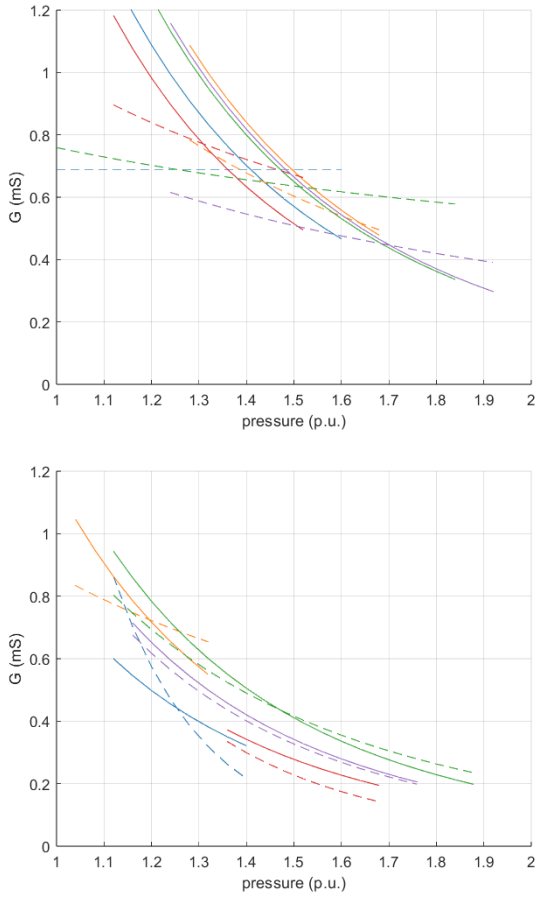

Figure 7. Comparison of the conductance-pressure fit based on preened method - solid line and exponential fitting with two parameters - dashed line. Measurements sereis with higher G200 values are plotted on top plot and with lower values on bottom.

values, which also exhibited lower scatter. In all cases, better agreement is observed over an intermediate pressure range compared to the extreme regions, possibly suggesting more complex pressure dependence. The results show that the pressure scaling exponent presented by Christen *et al.* agrees more closely with the present results compared to the exponent determined by Engelbrecht *et al.*. It may be that part of this difference can be attributed to the low range of pressures investigated in [6].

One factor limiting the accuracy of this method could be ablation of the nozzle and the arcing contacts, which changes the arcing zone geometry over the measurement series. Ablation leads to an increasing nozzle diameter, resulting in lower pressure at current zero - which is accounted for by the pressure dependence incorporated by the method. What is not represented is the change of gas flow conditions, which becomes less optimal and can affect cooling efficiency, potentially causing deviation in results.

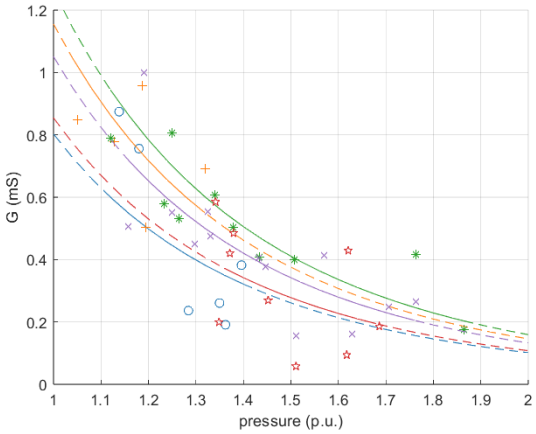

Figure 8. G200 values in function of the pressure, colors represent different measurement series, markers show single measurements, and lines are fitted based on equation 5 - solid line drawn in the region of measured pressures and extrapolation is drawn with dashed line

4. Conclusions

Limit values of G200 have been investigated for a large number of test object variants filled with CO_2/O_2 gas mixture under SLF L90-like test conditions. It was found that the overall limit is equal to 0.42 mS, with a standard deviation of $\sigma = 0.24$ mS.

Investigation of the dependence of G200 values on the pressure at current zero showed that the relation $G_{200} \sim \frac{1}{e^{\sqrt{p}}}$ gives a good description for the test object variants that yielded the lowest G200 values. For the measurement series where the G200 values were higher and more scatter was observed, this relation was closer to $G_{200} \sim \frac{1}{e^{p^{1/3}}}$.

References

[1] R. Smeets et al. New Arc Parameter Database for Characterisation of Short-Line Fault Interruption Capability of High-Voltage Circuit Breakers. In *2006 CIGRE Paris Session*, number A3-110, 2006.

[2] M. Seeger. "Environmentally friendly high-voltage AC switching technology: gas circuit breakers with SF6 alternative gases". In K. Niayesh, editor, *Green HV Switching Technologies for Modern Power Networks*, pages 227–312. IET, London, UK, 2023. doi:10.1049/PBPO236E_ch4.

[3] P. Pietrzak, J. Engelbrecht, D. Kumari, and C. M. Franck. Short-line fault switching performance comparison of SF_6 alternatives. *IEEE Transactions on Power Delivery*, 39(6):3071–3081, 2024. doi:10.1109/TPWRD.2024.3451178.

[4] D. Schiffbauer et al. High Voltage F-gas Free Switchgear applying CO_2 /O_2 Sequestration with a Variable Pressure Scheme. In *CIGRE-IEC 2019 Conference on EHV and UHV (AC & DC)*, 2019.

[5] T. Christen and M. Seeger. Current interruption limit and resistance of the self-similar electric arc. *Journal of Applied Physics*, 97(10):106108, 05 2005. doi:10.1063/1.1913802.

[6] J. T. Engelbrecht, D. Kumari, P. Pietrzak, and C. M. Franck. Thermal current interruption in CO_2-based mixtures: I. evaluating parameter dependence. *Journal of Physics D: Applied Physics*, 58(22):225503, may 2025. doi:10.1088/1361-6463/adcf33.

[7] T. Votteler and P. Stoller. Electronic circuit for measuring the current slope (dI/dt) and the post-arc current in gas-filled circuit breakers. *Review of Scientific Instruments*, 91(2), 2020. doi:10.1063/1.5125232.

[8] U. Habedank and H. Knobloch. Zero-crossing measurements as a tool in the development of high-voltage circuit breakers. 148(6):268–272, 2001. doi:10.1049/ip-smt:20010585.